PAPER
Ikuna Kanehara *et al.*
Local infrared spectral measurement system for the inspection of independent nano-plastic particles in water-based solutions

PAPER

Check for updates

Local infrared spectral measurement system for the inspection of independent nano-plastic particles in water-based solutions†

Ikuna Kanehara, [iD] *[a] Tatsuhiro Nagasaka,‡[b] Hirofumi Seki,‡[b] Sho Fujii,‡[c] Tsuyoshi Kimura, [iD] ‡[d] Masaya Yamamoto [iD] ‡[e] and Tadao Tanabe[a]

This study proposes a new method of bubble accumulation that enables the capture of individual nanoparticles diluted in water-based solvent and the evaluation of the shape and local infrared spectra of each independent nanoparticle. We have demonstrated this system using nanoparticles of defined size generated by nano-second laser ablation. Following a process of concentration of microbubbles, we have been able to analyze the material properties of individual nanoparticles by AFM-IR. The AFM images and IR spectra results indicate the presence of independent nanoparticles, and the IR spectra showed that the particle size is considered to decrease as the oxidation reaction progresses. This system approach for the concentration and analysis of nanoparticles can particularly contribute to bio adaptation research, since the identification of the physical properties of nanoparticles can provide a better understanding of the environmental/biological effects and relationships, the mechanism of nanoparticle aggregation and the interatomic forces between particles.

Environmental significance

Currently, micro-plastics floating in the ocean are misidentified as phytoplankton or seaweed and bioaccumulated through the food chain, potentially causing chronic health effects on apex predators. The biological effects and nanophysical properties of nano-plastics, which are much smaller in size than micro-plastics, are not well understood. It is also difficult to measure and analyze the morphology and physical properties of nano-plastics collected from nature. For low molecular weight polyethylene with nano-sized particles whose size is defined by laser ablation, this study reports on the analytical processing design to provide the accumulation of nano-plastics diluted in water-based solvents and evaluation of their individual IR spectral properties. Identifying the physical properties of nanoparticles could be one means of solving environmental problems through a better understanding of environmental and nanotoxicology and relationships, aggregation mechanisms, and interatomic forces between particles.

1 Introduction

Currently, methods for the identification of micro-plastics (MPs, 1 μm–5 mm in size)[1,2] floating in the ocean can

[a] Department of Engineering and Design, Shibaura Institute of Technology, 3-7-5, Toyosu, Koto-ku, Tokyo, 135-8548, Japan. E-mail: md23041@shibaura-it.ac.jp, tanabet@shibaura-it.ac.jp; Fax: +81 3 5859 8401; Tel: +81 3 5859 8828
[b] Toray Research Center, Inc., 2-11, Sonoyama 3-chome, Otsu, Shiga, 520-8567, Japan. E-mail: tatsuhiro.nagasaka.w5@trc.toray, hirofumi.seki.h9@trc.toray
[c] Faculty of Science, Yamagata University, 1-4-12 Kojirakawa, Yamagata, 990-8560, Japan. E-mail: sfujii@sci.kj.yamagata-u.ac.jp
[d] Department of Biomedical Engineering, Faculty of Life Science, Toyo University, 48-1 Oka, Asaka-shi, Saitama, 351-8510, Japan. E-mail: kimura007@toyo.ac.jp
[e] Department of Materials Processing, Graduate School of Engineering, Tohoku University, 6-6-02 Aramaki-aza Aoba, Aoba-ku, Sendai, 980-8579, Japan. E-mail: masaya.yamamoto.b6@tohoku.ac.jp

† Electronic supplementary information (ESI) available. See DOI: https://doi.org/10.1039/d4en00379a
‡ These authors contributed equally to this work.

misidentify these as phytoplankton or seaweed. When ingested by sea-life, such MPs can bioaccumulate through the food chain, with the potential for chronic health effects on apex predators.[1–29] Whilst a great deal of research around the world has studied the interaction of MPs with biological systems, their toxicity, the formation mechanisms, and an understanding of the biological effects and nano-physical properties of nano-plastics (NPs, 1 nm–1 μm in size),[2,14–16] which are much smaller in size than MPs, are not fully understood. Further research on NPs needs to be conducted as soon as possible. However, it is difficult to collect NPs dispersed in nature, and to measure and analyze their morphology and material properties. Therefore, in order to advance our understanding of biological effects in NPs, it is necessary not only to artificially create model samples of dispersed NPs,[3–6] but also to clarify the physical and chemical properties of individual artificially created NPs.

i) Preparation of nanoparticles: many studies have used polystyrene nano-plastics (PS-NPs, monodisperse, smooth and spherical in morphology) for applied studies of interactions with biological systems and toxicity.[4,17,18] However, because of their different properties from other polymers, and because they differ significantly from the rough surfaces and irregular shapes of their natural counterparts, these PS-NPs lack relevance to the environment and cannot represent realistic NPs in the environment.[4,17,18] In addition, the presence of solvent residues, surfactants, and impurities make it inappropriate to use NPs produced by liquid-phase synthesis or pulverization for applied studies of interactions with biological systems and toxicity.[3] In contrast, it is becoming possible to use laser ablation to produce model samples of NPs that are artificially dispersed in nature, free of solvent residues, surfactants, and impurities. Magrì (2018) *et al.* performed nano-second laser ablation (irradiation wavelength 248 nm, pulse duration 20 ns, repetition frequency 20 Hz, Coherent-CompexPro 110) on a commercial PET film (Goodfellow Cambridge Ltd) in Milli-Q water under an irradiation fluence of 4.5 J cm^{-2} and with an ablation area of 4 cm^2. The average particle size of the generated PET-NPs was 26.7 ± 14.2 nm.[6] It is also becoming clear that the conditions under which laser ablation is performed can control the particle size.[3] Kanehara (2023) *et al.* performed nano-second laser ablation (irradiation wavelength 266 nm, pulse duration 12–15 ns, repetition frequency 10 Hz, Lotis Tii LS-2134D) on a reagent LDPE film (Sigma-Aldrich Co. LLC) in ultra-pure water under an irradiation fluence of 8.0 mJ cm^{-2} for 0.5–1.5 h on a 0.023 cm^2 area. As a result, it was found that the longer the laser irradiation time, the smaller the particle size of NPs in the generated LDPE.[3] Typical concentrations of micro/nano plastics in the environment range from a few dozen of particles m^{-3} [30] to more than 1000 particles m^{-3},[31,32] but the concentration of the model nanoparticles produced is only 10^8 particles per ml,[3] which is not sufficient for the particle concentration needed to measure biotoxicity and bio immunity.[33,34]

ii) Collection: concentration by centrifugation methods is not applicable due to the possibility of condensation, transformation, and non-dispersibility of the fine particles. In addition to centrifugation methods, other NP collection methods include membrane filtration, field flow fractionation, cloud point extraction, pressurized fluid extraction, alkali-assisted thermal hydrolysis,[18] and emulsions,[19] but none of these methods are suitable for NPs extraction because of the difficulty of separating and identifying NPs from sand and organic contaminants[20] (see the ESI† for the advantages and disadvantages of each method for collecting nanoscale plastic particles (Table S1†)). Although the dilute state is not suitable for measurement, the dilute state makes it possible to evaluate a single particle. It is expected that Marangoni convection created by bubbles could be used to properly analyze fine particles.[35–37] The study has reported that marine nano-samples are actually concentrated and accumulated at the microbubble interface by inducing Marangoni convection through the generation of microbubbles by focused laser heating at the interface between the substrate and the sample solution.[38]

iii) Physical and chemical analysis: for the evaluation of NPs, a standard physical property evaluation such as shape observation by electron microscopy, average particle size evaluation by DLS, chemical characterization by Raman spectroscopy, and acquisition of infrared spectra of aggregated nanoparticles by FTIR are mainly studied.[19–21] However, these physical and chemical analysis methods are limited in their ability to characterize the presence of such particles in liquid samples[22–26] (see the ESI† for the advantages and disadvantages of each method for visual and spectral analyzing nanoscale plastic particles (Table S2 and S3†)). Ecological studies using micro- and nanoparticles of polystyrene (PS), which are easy to fabricate with uniform particle size and shape, have been conducted worldwide,[26–29] and PET-NPs, a crystalline plastic other than PS, has only been found to pass through intestinal epithelial cells.[6] Thus, studies on the aggregate and standard physical properties of particles and their biological effects have been initiated, but the physical properties of individual NPs themselves remain unexplored. Although IR spectroscopy has been widely used to evaluate the physical properties of polymers, it is difficult to evaluate the chemical properties of nanoparticles due to the limitation of spatial resolution, which only provides an average IR spectrum for many particles with a spatial resolution of several micrometers or more. Recently, however, AFM-IR has been developed as a nano IR spectroscopy method by Dazzi *et al.*[39–43] AFM-IR is a technique in which light from a tunable infrared laser is irradiated onto a localized region of a sample and the resulting amplitude change in photothermal expansion of the sample is measured using the cantilever of an atomic force microscope to obtain IR absorption spectra and absorption images of individual independent particles with a spatial resolution on the 50–100 nm scale.[39–45] Although the concentration of NPs produced by laser ablation is highly dilute and needs to be concentrated, the physical properties of individual NPs can be potentially evaluated by allowing independent particles to accumulate without aggregation on the prism used in AFM-IR.

As yet, the processes involved in this study have been developed independently and have not been optimised as a complete method. This study proposes and demonstrates a new method to evaluate NPs to measure the shape and local infrared properties of concentrated nanoparticles by adapting bubble accumulation, as shown in Fig. 1. Our method realizes the capture of individual nanoparticles diluted in solvent and will be available for the study of biological effects. Once the physical properties of the nanoparticles themselves are clarified, a better understanding of the environmental and biological effects and relationships, the mechanism of NP aggregation, and the interatomic forces between particles can be promoted based on the correct nanoparticle properties.

2 Experimental

In order to develop a new method that can evaluate the local infrared spectral properties of nanoparticles by adapting bubble collection, three processes need to be optimised.
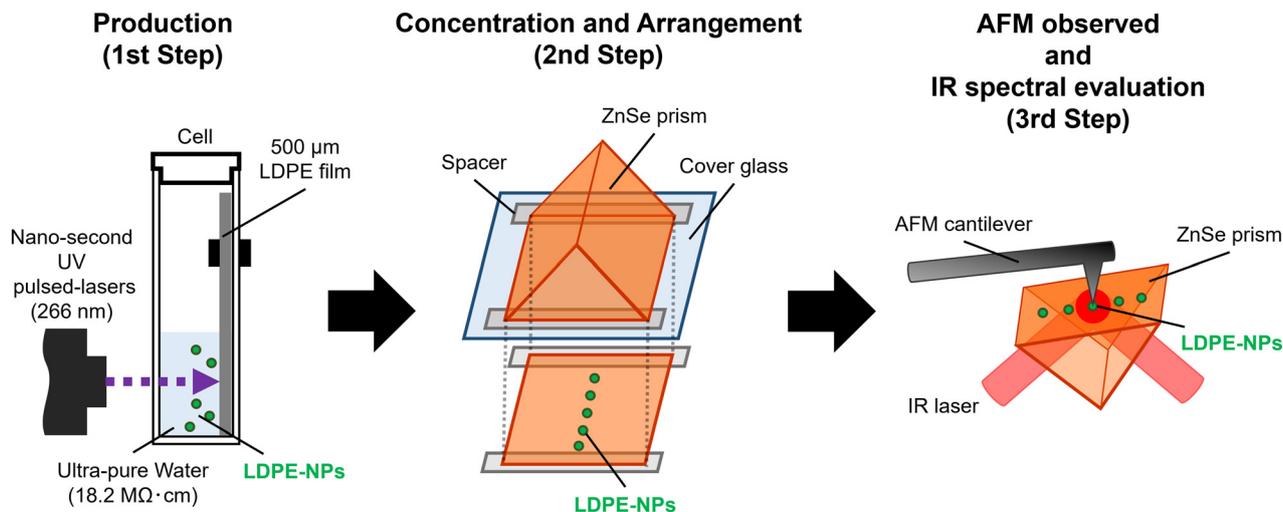
1108 | *Environ. Sci.: Nano*, 2025, **12**, 1107–1115

This journal is © The Royal Society of Chemistry 2025

Fig. 1 Schematic of our system designed to evaluate the local infrared spectral properties of nanoparticles by adapting bubble accumulation to capture individual nanoparticles diluted in solvent.

Firstly, appropriate nanoparticles need to be produced by nano-second laser ablation. The conditions we have used are shown in Table 1. A double pulsed Q-switched Nd:YAG laser (Irradiation wavelength 266 nm, Pulse duration of 12–15 ns, Repetition rate of 10 Hz, Lotis Tii LS-2134D) is used. It consists of two independent Nd:YAG lasers pumped by a single flash lamp. A 500 μm thick LDPE film sample (Aldrich LDPE (melt index 25 g/10 min (190 °C/2.16 kg)), Sigma-Aldrich Co. LLC) is fixed inside a quartz glass cell filled with ultrapure water (18.2 MΩ cm, Simplicity UV). There, a laser

Table 1 The Nano-second laser ablation conditions for producing suitable nanoparticles

Material		Aldrich LDPE (melt index 25 g/10 min (190 °C/2.16 kg))
Shape of the material		500 μm film
Laser		A double pulsed Q-switched Nd:YAG laser (Lotis Tii LS-2134D)
Specifications of laser	Pulse duration	12–15 ns
	Repetition rate	10 Hz
	Irradiation wavelength	266 nm
	Output energy	0.91 mJ
	Shooting area	0.023 cm^2
	Energy density	40 mJ cm^{-2}
	Irradiation time	1.0 h
Cell	Type	Full-sided clear
	Optical path length	10 mm
	Capacity	3.5 ml
	Size	12.5 × 12.5 × 56 mm
	Material	Quartz glass
	Model number	SC10104
	Transmittance at 266 nm	90%
Fluence on sample surface		36 mJ cm^{-2}
Dispersing solvent	Water	Ultra-pure water
	Electrical resistivity	18.2 MΩ cm

beam with a UV wavelength of 266 nm is irradiated for 1 h on the LDPE film sample, and NPs are produced.

In the second process, the NPs produced by nano-second laser ablation in the above are concentrated to analyze the local chemical properties of one particle using microbubbles and placed one particle at a time on a zinc selenide (ZnSe) substrate.[46] Normally, ITO substrates are applied. The laser-induced microbubbles on the Au film (10 nm) or ITO substrate were formed with 1064 nm irradiation because the substrates absorb the wavelength of 1064 nm and provide photothermal effect.[35–37] However, in this study, ZnSe prisms were chosen to avoid the influence of infrared absorption in the AFM-IR measurements. For ZnSe, absorption of light occurs at less than 600 nm. In addition, thermal conductivity of ZnSe (18 Wm^{-1} K^{-1}) is similar to that of the Au film (38.5 Wm^{-1} K^{-1}) and ITO (50 Wm^{-1} K^{-1}). Therefore, irradiation with a 450 nm laser (~45 mW) leads to the formation of the bubble.

Fig. 2 shows a model diagram of the enrichment method using microbubbles. Two pieces of extended Parafilm (thickness: ~40 μm) as spacers placed on a cover glass, and a ZnSe prism (Nihon Thermal Consulting. Co) was placed on the spacers with its surface to be measured by AFM-IR facing inward. Then, the chamber constructed with the prism was placed on the stage of an inverted optical microscope (IX 71, Olympus), equipped with an oil-immersion objective lens (×100/1.30 NA, Olympus). The solution containing LDPE-NPs by nano-second laser ablation was introduced into the chamber by capillary action. A continuous wave (CW) light beam (450 nm) from a diode laser (Civil Laser) was focused on the ZnSe prism surface through the objective lens of the microscope. The laser intensity at 450 nm was monitored before passing the beam through the objective lens. The focus point of the laser beam was controlled by x–y stage movement of the microscope. Microscopy images were recorded on a CMOS camera (WRAYCAM-VEX120, WRAYMER) mounted on the microscope.

This journal is © The Royal Society of Chemistry 2025

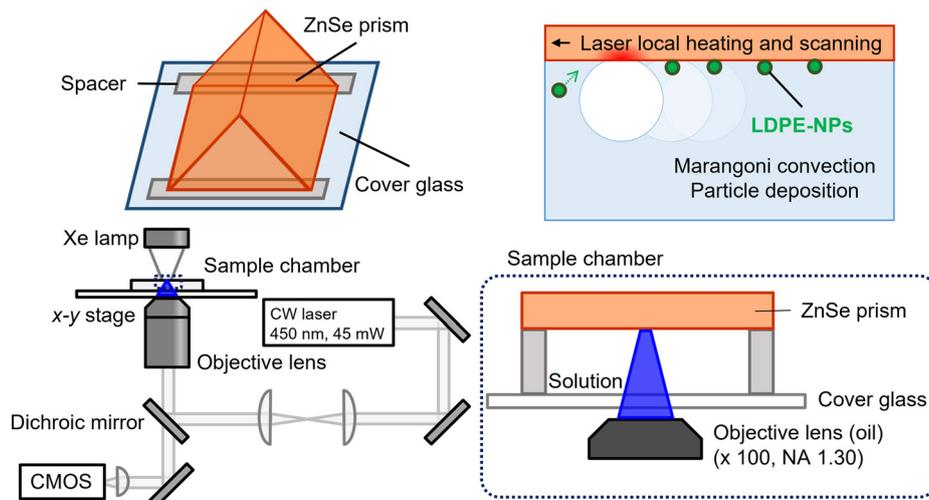*Environ. Sci.: Nano*, 2025, **12**, 1107–1115 | **1109**

Fig. 2 Schematic of the collection method of LDPE–NPs using microbubbles. The diameter of microbubbles obtained was 5–10 μm.

Finally, nanoIR (Anasys Instruments)[47] AFM-IR is used to obtain the infrared spectra of the individual nanoparticles. The nanoIR system uses a pulsed, wavelength-variable IR source to analyze the individual pumped molecular vibrations within the LDPE-NPs. As in conventional ATR spectroscopy, the IR beam is irradiated onto the LDPE-NPs by total internal reflection, and rapid thermal expansion occurs as the LDPE-NPs absorb the energy. The cantilever vibrations induced by the thermal expansion are damped by a characteristic ring down, and the amplitude and frequency of the vibrations are extracted by Fourier transform.[47] Next, the local IR absorption spectrum of LDPE-NPs is obtained by measuring the amplitude of the cantilever vibration while sweeping the wavelength of the irradiating IR laser.

3 Results and discussion

Fig. 3(a) shows the particle size distribution of LDPE-NPs generated from nano-second laser ablation against the dynamic light scattering (DLS) intensity for 1.0 h (3.6×10^4 pulses) laser exposure time. Fig. 3(b) shows the graph of the autocorrelation function. The autocorrelated polystyrene latex particles (100.5 ± 2.6 nm, monodispersed) at a concentration of 10 mg ml^{-1} are shown as a black line as a reference in the DLS measurement.

The particle size distribution against the scattering intensity in Fig. 3(a) shows that the particle size of LDPE-NPs generated by nano-second laser ablation is distributed in the range of 50–500 nm, and that LDPE-NPs with a diameter of 200 nm are particularly abundant. However, the graph of the autocorrelation function in Fig. 3(b) shows that the value of the autocorrelation function is smaller than that of the polystyrene latex particles in the reference, suggesting that the number of generated LDPE-NPs particles is still rather small. This strongly indicates the need for microbubble accumulation in this study.

Fig. 4(a) shows an optical image of the bubble generation by 450 nm laser irradiation on the ZnSe prism surface. The
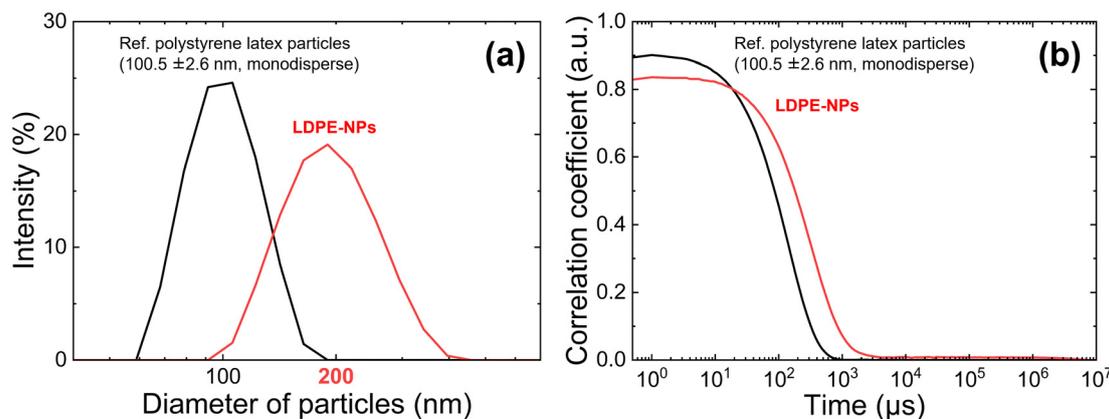

Fig. 3 Particle size evaluation of LDPE-NPs by DLS measurement. Polystyrene latex particles (100.5 ± 2.6 nm, monodisperse) at a concentration of 10 mg mL^{-1} are shown as a black line as a reference. (a) Particle size distribution by scattering intensity *versus* laser irradiation time of 1.0 h (3.6 × 10^4 pulses) and (b) graph of the autocorrelation function.

1110 | *Environ. Sci.: Nano*, 2025, **12**, 1107–1115

This journal is © The Royal Society of Chemistry 2025

ZnSe prism was irradiated with a 450 nm laser to induce a photothermal effect, which generated microbubbles in the solvent with micro- and nano-plastic particles, and the micro- and nano-plastic particles were collected by Marangoni convection. After the laser irradiation was stopped and the bubbles disappeared, the substrate surface was observed, and no holes or other damage was found on the substrate. For reference, an aqueous solution in which polyethylene particles 1–4 μm in diameter (Ref. PE-MPs, CPMS-0.96 1–4 μm–0.2 g, Cospheric) were dispersed and introduced into the chamber to generate the bubbles, and the Ref. PE-MPs gathered around the bubbles and accumulated on the surface of the ZnSe substrate (Fig. 4(b)). These demonstrations on the ZnSe substrate show that the previously reported bubble enrichment and collection of micro- and nanoparticles is also possible on the ZnSe substrate and can be deployed in a combined AFM-IR measurement system. Unfortunately, nano-sized plastic particles cannot be observed under an optical microscope, but they are assumed to have accumulated, and samples were then prepared for AFM-IR spectral measurements.

Fig. 5 shows the IR spectra of the LDPE-NPs prepared on the ZnSe prism, along with AFM images of the micro-particles that were present in the observation area. The IR spectrum of Ref. PE-MPs used as a reference is also shown. PE-MPs were focused on a ZnSe prism, and the IR spectra were measured from nanoIR.

The AFM image of the nanoparticles and the IR spectra (Fig. 5) confirm that the LDPE particles are not only independently spherical and nano-sized (Fig. 5(A)), but also that some LDPE particles are distorted or agglomerated in shape or exist in aggregates, as seen in Fig. 5(B) and (C). (see the ESI† for the height profiles of (A) LDPE-NPs of about 300 nm diameter, (B) LDPE-MPs.1, and (C) LDPE-MPs.2 (Fig. S1†)). The IR spectra show signals originating from C=O stretching (1735 cm^{-1}), C–O stretching (1240 cm^{-1}, 1165 cm^{-1}), C=C stretching (1600 cm^{-1}, 1580 cm^{-1}), and O–H stretching (3400 cm^{-1}), confirming the progress of the oxidation reaction.[46] In particular, CH$_2$ asymmetric C–H stretching (2918 cm^{-1}), CH$_2$ symmetric C–H stretching (2848 cm^{-1}), CH$_3$ asymmetric stretching (2960 cm^{-1}), and CH$_3$ symmetric stretching (2870 cm^{-1}) can be also found following

the oxidation reaction. This is thought to be due to the formation of the terminal methyl group.[48–51] In addition, the methyl group shows a peak at a higher wavenumber than the methylene group in the IR spectra of polypropylene with both methyl and methylene groups.[48–51] Furthermore, in LDPE-NPs with a diameter of about 300 nm (Fig. 5(A)), the peak intensity of the C=C bond increased compared to that of the C=O bond, and a lower wavenumber shift was observed compared to the C=C bond of mono-olefins, suggesting the formation of relatively long conjugated systems. It is thought that the photo-oxidation first occurs on the surface of micro- and nano-plastics (MNPs) and produces highly reactive organic radicals and ROS that are involved in the radical reactions.[52] Typically, along with the generation of alcohols, ketones, olefins, and aldehydes, carboxylic acids and eaters, vinyl groups and O-containing functional groups, such as carbonyl, carboxyl, and hydroxyl groups can be formed during the photo-oxidation of MNPs.[52] In addition, new peaks in the carbonyl (1500–1800 cm^{-1}) and hydroxyl (3000–3800 cm^{-1}) regions were observed in UV-irradiated polypropylene-microplastics (PP-MPs) in ultrapure water, indicating the formation of oxygen related functional groups on the surface of PP-MPs during the aging process from ATR-FTIR analysis.[53] Please refer to the ESI† for an example of a possible decomposition reaction scheme (Fig. S2†). Note that for Ref. PE-MPs, standard PE absorption spectra are obtained. This suggests that the oxidation was promoted by nano-second laser ablation at ultraviolet wavelengths or in ultrapure water, and not by laser-induced oxidation at the time of accumulation.[54–60] From the above, we confirmed the relation between the size and state of the nanoparticles. One of the most possible explanations is that greater oxidation produces smaller particles.

4 Conclusions

This study proposes and demonstrates a new method to evaluate the shape and local infrared properties of nanoparticles by adapting bubble accumulation, which achieves the capture of individual nanoparticles diluted in solvent. Three steps are completed: first, nano-second laser ablation is utilized to fabricate nanoparticles to fabricate a
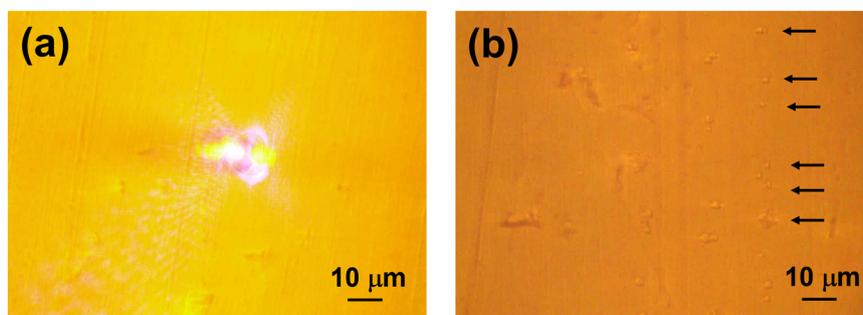

Fig. 4 Optical images of the interface between the ZnSe prism surfaces and solution under a microscope. (a) Generation of a microbubble by 450 nm laser irradiation and (b) ref. PE–MPs (1–4 μm) deposited by the bubble. Black arrows indicate some of the particle locations.
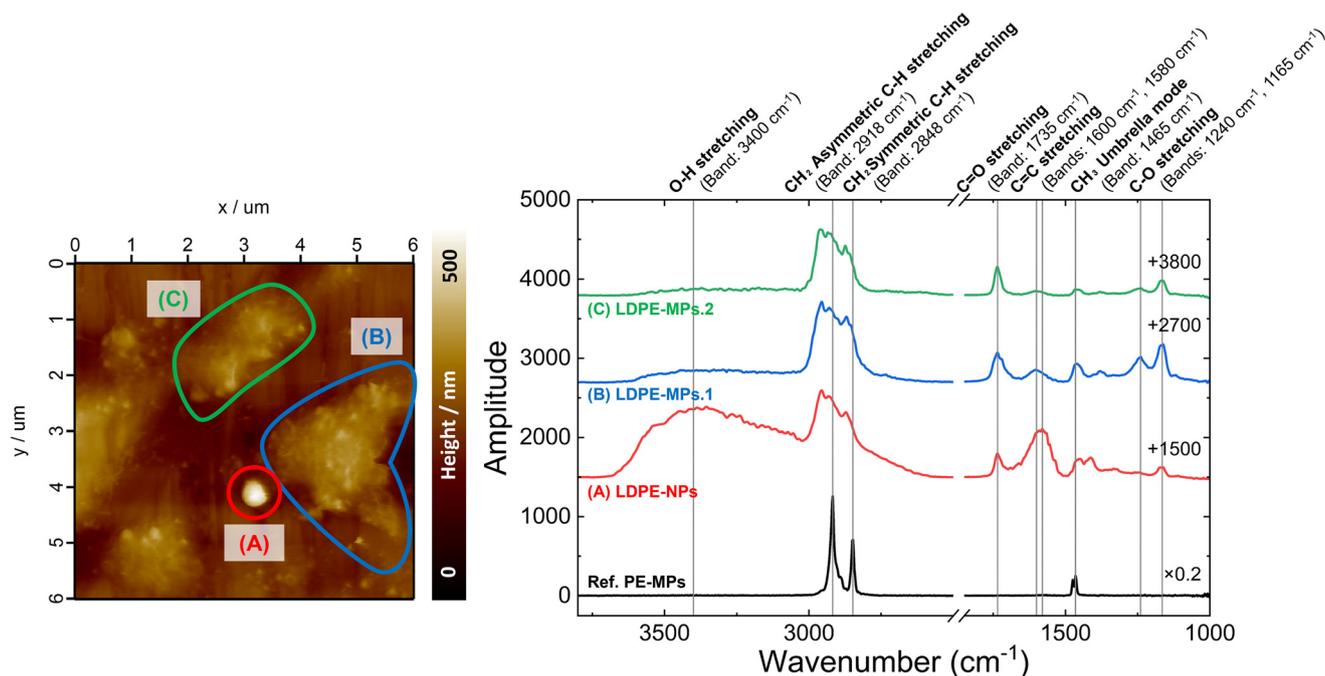
This journal is © The Royal Society of Chemistry 2025

Environ. Sci.: Nano, 2025, **12**, 1107–1115 | 1111

Fig. 5 AFM images and IR spectra of nanoparticles. It was found that the particle size is considered to decrease as the oxidation reaction progresses. (A) LDPE-NPs of about 300 nm diameter, (B) LDPE-MPs.1 and (C) LDPE-MPs.2.

defined model sample that is artificially dispersed in nature without solvent residues, surfactants, or impurities. The specific conditions were as follows: nano-second laser ablation (irradiation wavelength of 266 nm, pulse duration of 12–15 ns, repetition rate of 10 Hz, an irradiation fluence of 36 mJ cm^{-2}, and an ablation area of 0.023 cm^2) for a 500 μm thick LDPE film sample was performed; second, LDPE-NPs were concentrated and prepared to analyze the local chemical properties of single particles. Using Marangoni convection of microbubbles, LDPE-NPs were placed one particle at a time on the ZnSe substrate surface. Thirdly, AFM-IR of nanoIR (Anasys Instruments)[47] was used to analyze the chemical properties of nanoparticles as well as shape observations for individual nanoparticles. AFM observations confirmed the presence of independent nanoparticles. For these, infrared resonance peaks attributed to C=O stretching, C–O stretching, C=C stretching, O–H stretching, *etc.* were observed, confirming the progress of the oxidation reaction. For nanoparticles with a diameter of about 300 nm, the intensity of the C=C bond increased compared to the C=O bond, and a red shift was observed compared to the C=C bond of mono-olefins, suggesting the formation of relatively long conjugated systems.

Based on these results, whilst the formation mechanism, understanding of biological effects, and nano-physical properties in NPs dispersed in natural solutions have not been clarified, this study significantly advances the processes of NP generation, preparation, and analysis. This system design approach, as proposed in Fig. 1, can contribute to NP research as a system for rapid generation, concentration, and analysis. The clarification of the physical properties of the nanoparticles will help to better understand their environmental and biological effects and relationships, the mechanism of NP aggregation, and the interatomic forces between particles.

Data availability

The data supporting this article have been included as part of the ESI.†

Author contributions

Ikuna Kanehara: investigation (lead); visualization (equal); formal analysis (equal); writing – original draft (lead); writing – review and editing (equal). Tatsuhiro Nagasaka: resources (lead); formal analysis (equal); writing – review and editing (equal). Hirofumi Seki: resources (supporting); formal analysis (supporting); writing – review and editing (equal). Sho Fujii: visualization (equal); formal analysis (equal); writing – original draft (supporting); writing – review and editing (equal). Tsuyoshi Kimura: supervision (equal); writing – review and editing (equal). Masaya Yamamoto: supervision (lead); funding acquisition (lead); writing – review and editing (equal). Tadao Tanabe: supervision (equal); writing – original draft (supporting); writing – review and editing (equal).

Conflicts of interest

The authors have no conflicts to disclose.

Acknowledgements

References

1 N. I. B. Hartmann, T. Nolte, M. A. Sørensen, P. R. Jensen and A. Baun, Aquatic ecotoxicity testing of nanoplastics: lessons learned from nanoecotoxicology, *ASLO Aquat. Sci. Meet.*, 2015, vol. 2015, Sound/Visual production (digital), DTU Environment.

2 H. T. Shiu, X. Pan, Q. Liu, K. Long, K. K. Y. Cheng, B. C. B. Ko, J. K. H. Fang and Y. Zhu, Dietary exposure to polystyrene nanoplastics impairs fasting-induced lipolysis in adipose tissue from high-fat diet fed mice, *J. Hazard. Mater.*, 2022, **440**, 129698, DOI: **10.1016/j.jhazmat.2022.129698**.

3 I. Kanehara, H. Yamashita, S. Fujii, T. Kimura, M. Yamamoto and T. Tanabe, Nano-Sized Polyethylene Particles Produced by Nano-Second UV Laser Ablation, *Lasers Manuf. Mater. Process.*, 2023, **10**, 389–399, DOI: **10.1007/s40516-023-00214-9**.

4 S. Hiranphinyophat, T. Hiraoka, M. Kobayashi, S. Fujii, A. Kishida, T. Tanabe, T. Kimura and M. Yamamoto, Fabrication of Polypropylene Nanoplastics Via Thermal Oxidation Reaction for Human Cells Responsiveness Studies, *Langmuir*, 2023, **39**, 15563–15571, DOI: **10.1021/acs.langmuir.3c01858**.

5 N. Washihira, M. Murakami, M. Nakamura, S. Fujii, T. Matsushima, H. Asahara, A. Kishida, T. Tanabe, T. Kimura, M. Kobayashi and M. Yamamoto, Application of a genetically engineered macrophage cell line for evaluating cellular effects of UV/US-treated poly (ethylene terephthalate) microplastics, *Colloids Surf., B*, 2024, **234**, 113735, DOI: **10.1016/j.colsurfb.2023.113735**.

6 D. Magrì, M. P. Sánchez, G. Caputo, F. Gatto, M. Veronesi, G. Bardi, T. Catelani, D. Guarnieri, A. Athanassiou, P. P. Paolo and D. Fragouli, Laser Ablation as a Versatile Tool To Mimic Polyethylene Terephthalate Nanoplastic Pollutants: Characterization and Toxicology Assessment, *ACS Nano*, 2018, **12**(8), 7690–7700, DOI: **10.1021/acsnano.8b01331**.

7 T. Luo, S. Moon, L. Martin, S. Kim, Q. Zhang and W. Xu, Direct Observation of Nanoplastics in Ocean Water, *ChemRxiv*, Cambridge Open Engage, Cambridge, 2023, preprint, DOI: **10.26434/chemrxiv-2023-375jp**.

8 C. Waymana and H. Niemann, The fate of plastic in the ocean environment – a minireview, *Environ. Sci.: Processes Impacts*, 2021, **23**, 198–212, DOI: **10.1039/D0EM00446D**.

9 B. Gewert, M. M. Plassmanna and M. MacLeod, Pathways for degradation of plastic polymers floating in the marine environment, *Environ. Sci.: Processes Impacts*, 2015, **17**, 1513–1521, DOI: **10.1039/C5EM00207A**.

10 F. R. Khan, K. Syberg, Y. Shashoua and N. R. Bury, Influence of polyethylene microplastic beads on the uptake and localization of silver in zebrafish (Danio rerio), *Environ. Pollut.*, 2015, **206**, 73–79, DOI: **10.1016/j.envpol.2015.06.009**.

11 J. Duan, Y. Li, J. Gao, R. Cao, E. Shang and W. Zhang, ROS-mediated photoaging pathways of nano- and micro-plastic particles under UV irradiation, *Water Res.*, 2022, **216**, 118320, DOI: **10.1016/j.watres.2022.118320**.

12 L. Cai, J. Wang, J. Peng, Z. Wu and X. Tan, Observation of the degradation of three types of plastic pellets exposed to UV irradiation in three different environments, *Sci. Total Environ.*, 2018, **628–629**, 740–747, DOI: **10.1016/j.scitotenv.2018.02.079**.

13 V. P. Ranjan and S. Goel, Degradation of Low-Density Polyethylene Film Exposed to UV Radiation in Four Environments, *J. Hazard., Toxic Radioact. Waste*, 2019, **23**(4), DOI: **10.1061/(ASCE)HZ.2153-5515.0000453**.

14 N. B. Hartmann, T. Hüffer, R. C. Thompson, M. Hassellöv, A. Verschoor, A. E. Daugaard, S. Rist, T. Karlsson, N. Brennholt, M. Cole, M. P. Herrling, M. C. Hess, N. P. Ivleva, A. L. Lusher and M. Wagner, Are We Speaking the Same Language? Recommendations for a Definition and Categorization Framework for Plastic Debris, *Environ. Sci. Technol.*, 2019, **53**, 1039–1047, DOI: **10.1021/acs.est.8b05297**.

15 J. Gigault, A. T. Halle, M. Baudrimont, P. Y. Pascal, F. Gauffre, T. L. Phi, H. E. Hadri, B. Grassl and S. Reynaud, Current opinion: What is a nanoplastic?, *Environ. Pollut.*, 2018, **235**, 1030–1034, DOI: **10.1016/j.envpol.2018.01.024**.

16 C. G. Alimba and C. Faggio, Microplastics in the marine environment: Current trends in environmental pollution and mechanisms of toxicological profile, *Environ. Toxicol. Pharmacol.*, 2019, **68**, 61–74, DOI: **10.1016/j.etap.2019.03.001**.

17 Q. Gao, Y. Wang, Y. Ji, X. Zhao, P. Zhang and L. Chen, Tracking of realistic nanoplastics in complicated matrices by iridium element labeling and inductively coupled plasma mass spectroscopy, *J. Hazard. Mater.*, 2022, **424**, 127628, DOI: **10.1016/j.jhazmat.2021.127628**.

18 P. Li, Q. Li, Z. Hao, S. Yu and J. Liu, Analytical methods and environmental processes of nanoplastics, *J. Environ. Sci.*, 2020, **94**, 88–99, DOI: **10.1016/j.jes.2020.03.057**.

19 Y. Li, J. Fu, L. Peng, X. Sun, G. Wang, Y. Wang and L. Chen, A sustainable emulsion for separation and Raman identification of microplastics and nanoplastics, *Chem. Eng. J.*, 2023, **469**, 143992, DOI: **10.1016/j.cej.2023.143992**.

20 H. Wang, Q. Wang, M. Lv, J. Li, X. Zhao, Z. Song, X. Wang, J. You, Y. Wang and L. Chen, Marine micro(nano)plastics determination and its environmental toxicity evaluation, *TrAC, Trends Anal. Chem.*, 2023, **168**, 1117332, DOI: **10.1016/j.trac.2023.117332**.

21 P. Natalia, Ivleva: Chemical Analysis of Microplastics and Nanoplastics: Challenges, Advanced Methods, and Perspectives, *Chem. Rev.*, 2021, **121**(19), 11886–11936, DOI: **10.1021/acs.chemrev.1c00178**.

22 F. Ribeiro, D. M. Mitrano, C. Hacker, P. Cherek, K. Brigden, S. L. Kaserzon, K. V. Thomas and T. S. Galloway, Short Depuration of Oysters Intended for Human Consumption Is Effective at Reducing Exposure to Nanoplastics, *Environ. Sci. Technol.*, 2022, **56**(23), 16716–16725, DOI: **10.1021/acs.est.2c02269**.

23 X. Zhao, Y. Wang, Y. Ji, R. Mei, Y. Chen, Z. Zhang, X. Wang and L. Chen, Polystyrene nanoplastics demonstrate high

This journal is © The Royal Society of Chemistry 2025

Environ. Sci.: Nano, 2025, **12**, 1107–1115 | **1113**

structural stability in vivo: A comparative study with silica nanoparticles via SERS tag labeling, *Chemosphere*, 2022, **300**, 134567, DOI: **10.1016/j.chemosphere.2022.134567**.

24 Q. Zhang, Y. Liu, Y. Liang, Y. Wu, W. Zhang, D. Zhang, G. S. Guo, Z. Liu and X. Wang, Quantitative Analysis of Nanoplastics in Single Cells by Subcellular Chromatography, *Anal. Chem.*, 2023, **95**(26), 9739–9745, DOI: **10.1021/acs.analchem.2c05428**.

25 H. Du, Y. Wang, P. Zhang, R. Mei, Y. Ji, X. Zhao, Z. Zhang, J. Ma and L. Chen, Quantitative assessment of in vivo distribution of nanoplastics in bivalve Ruditapes philippinarum using reliable SERS tag-labeled nanoplastic models, *Nanoscale*, 2022, **14**, 7807–7816, DOI: **10.1039/D2NR00157H**.

26 S. Xiao, A. Filippini, M. Casadei, G. Caracciolo, L. Digiacomo and A. Rossetta, Fast and portable fluorescence lifetime analysis for early warning detection of micro- and nanoplastics in water, *Environ. Res.*, 2024, **244**, 117936, DOI: **10.1016/j.envres.2023.117936**.

27 R. Sussarellu, M. Suquet, Y. Thomas, C. Lambert, C. Fabioux, M. E. J. Pernet, N. L. Goïc, V. Quillien, C. Mingant, Y. Epelboin, C. Corporeau, J. Guyomarch, J. Robbens, I. P. Pont, P. Soudant and A. Huvet, Oyster reproduction is affected by exposure to polystyrene microplastics, *Proc. Natl. Acad. Sci. U. S. A.*, 2016, **113**(9), 2430–2435, DOI: **10.1073/pnas.1519019113**.

28 M. Yang and W. X. Wang, Recognition and movement of polystyrene nanoplastics in fish cells, *Environ. Pollut.*, 2023, **316**, 120627, DOI: **10.1016/j.envpol.2022.120627**.

29 M. Sendra, A. Saco, M. P. Yeste, A. Romero, B. Novoa and A. Figueras, Nanoplastics: From tissue accumulation to cell translocation into Mytilus galloprovincialis hemocytes. resilience of immune cells exposed to nanoplastics and nanoplastics plus Vibrio splendidus combination, *J. Hazard. Mater.*, 2020, **388**, 121788, DOI: **10.1016/j.jhazmat.2019.121788**.

30 K. Enders, R. Lenz, C. A. Stedmon and T. G. Nielsen, Abundance, size and polymer composition of marine microplastics ≥10μm in the Atlantic Ocean and their modelled vertical distribution, *Mar. Pollut. Bull.*, 2015, **100**(1), 70–81, DOI: **10.1016/j.marpolbul.2015.09.027**.

31 J. L. Xu, K. V. Thomas, Z. Luo and A. A. Gowen, FTIR and Raman imaging for microplastics analysis: State of the art, challenges and prospects, *TrAC, Trends Anal. Chem.*, 2019, **119**, 115629, DOI: **10.1016/j.trac.2019.115629**.

32 K. Pabortsava and R. S. Lampitt, High concentrations of plastic hidden beneath the surface of the Atlantic Ocean, *Nat. Commun.*, 2020, **11**, 4073, DOI: **10.1038/s41467-020-17932-9**.

33 K. M. Takeshita, Y. Iwaaki, T. M. Sinclair, T. I. Hayashi and W. Naito, Illustrating a Species Sensitivity Distribution for Nano- and Microplastic Particles Using Bayesian Hierarchical Modeling, *Environ. Toxicol. Chem.*, 2022, **41**(4), 954–960, DOI: **10.1002/etc.5295**.

34 K. Tanaka, Y. Takahashi, H. Kuramochi, M. Osako and G. Suzuki, Preparation of Nanoplastic Particles as Potential

35 S. Fujii, R. Fukano, Y. Hayami, H. Ozawa, E. Muneyuki, N. Kitamura and M. Haga, Simultaneous Formation and Spatial Patterning of ZnO on ITO Surfaces by Local Laser-Induced Generation of Microbubbles in Aqueous Solutions of [Zn(NH3)4]2+, *ACS Appl. Mater. Interfaces*, 2017, **9**(9), 8413–8419, DOI: **10.1021/acsami.6b16719**.

36 S. Fujii, K. Kobayashi, K. Kanaizuka, T. Okamoto, S. Toyabe, E. Muneyuki and M. Haga, Manipulation of Single DNA Using a Micronanobubble Formed by Local Laser Heating on a Au-coated Surface, *Chem. Lett.*, 2010, **39**, 92–93, DOI: **10.1246/cl.2010.92**.

37 S. Fujii, K. Kanaizuka, S. Toyabe, K. Kobayashi, E. Muneyuki and M. A. Haga, Fabrication and placement of a ring structure of nanoparticles by a laser-induced micronanobubble on a gold surface, *Langmuir*, 2011, **27**(14), 8605–8610, DOI: **10.1021/la201616s**.

38 S. Moon, L. M. A. Martin, S. Kim, Q. Zhang, R. Zhang, W. Xu and T. Luo, Direct observation and identification of nanoplastics in ocean water, *Sci. Adv.*, 2024, **10**(4), eadh1675, DOI: **10.1126/sciadv.adh1675**.

39 A. Dazzi, R. Prazeres, F. Glotin and J. M. Ortega, Local infrared microspectroscopy with a subwavelength spatial resolution using an AFM tip as a photothermal sensor, *Opt. Lett.*, 2005, **30**(18), 2388–2390, DOI: **10.1364/OL.30.002388**.

40 P. Nguyen-Tri, P. Ghassemi, P. Carriere, S. Nanda, A. A. Assadi and D. D. Nguyen, Recent Applications of Advanced Atomic Force Microscopy in Polymer Science: A Review, *Polymer*, 2020, **12**, 1142, DOI: **10.3390/polym12051142**.

41 A. Dazzi, C. B. Prater, Q. Hu, D. B. Chase, J. F. Rabolt and C. Marcott, AFM-IR: combining atomic force microscopy and infrared spectroscopy for nanoscale chemical characterization, *Appl. Spectrosc.*, 2012, **66**(12), 1365–1384, DOI: **10.1366/12-06804**.

42 A. Dazzi and C. B. Prater, AFM-IR: Technology and Applications in Nanoscale Infrared Spectroscopy and Chemical Imaging, *Chem. Rev.*, 2017, **117**(7), 5146–5173, DOI: **10.1021/acs.chemrev.6b00448**.

43 D. Kurouski, A. Dazzi, R. Zenobi and A. Centrone, Infrared and Raman chemical imaging and spectroscopy at the nanoscale, *Chem. Soc. Rev.*, 2020, **49**, 3315–3347, DOI: **10.1039/C8CS00916C**.

44 J. J. Schwartz, D. S. Jakob and A. Centrone, A guide to nanoscale IR spectroscopy: resonance enhanced transduction in contact and tapping mode AFM-IR, *Chem. Soc. Rev.*, 2022, **51**, 5248–5267, DOI: **10.1039/D2CS00095D**.

45 A. C. V. D. dos Santos, D. Tranchida, B. Lendl and G. Ramer, Nanoscale chemical characterization of a post-consumer recycled polyolefin blend using tapping mode AFM-IR, *Analyst*, 2022, **147**, 3741–3747, DOI: **10.1039/D2AN00823H**.

46 C. Campanale, I. Savino, C. Massarelli and V. F. Uricchio, Fourier Transform Infrared Spectroscopy to Assess the Degree of Alteration of Artificially Aged and Environmentally Weathered Microplastics, *Polymer*, 2023, **15**, 911, DOI: **10.3390/polym15040911**.

Standards for the Study of Nanoplastics, *Yakugaku Zasshi*, 2024, **144**(2), 165–170, DOI: **10.1248/yakushi.23-00152-1**.

1114 | *Environ. Sci.: Nano*, 2025, **12**, 1107–1115

This journal is © The Royal Society of Chemistry 2025

47 C. Prater, K. Kjoller and R. Shetty, Nanoscale infrared spectroscopy, *Mater. Today*, 2010, **13**(11), 56–60, DOI: **10.1016/S1369-7021(10)70205-4**.

48 N. B. Colthup, L. H. Daly and S. E. Wiberley, *Introduction to Infrared and Raman Spectroscopy*, Academic Press, 3rd edn, 1990, pp. 1–547.

49 T. Miyazawa, *Infrared absorption and molecular structure of polypropylene (Infrared absorption spectrum theory and applications-17-), Area of chemistry*, Special issue, Nankodo Co., Ltd., 1965, vol. 68, pp. 63–114, **https://ndlsearch.ndl.go.jp/books/R000000004-I8140925**.

50 H. Horiguti, *Illustrated list of infrared absorption: Basics and practice of organic structural chemistry*, Sankyo Shuppan Co., Ltd., 1977, pp. 1–402.

51 *PerkinElmer Co., Ltd.*, **https://www.perkinelmer.co.jp/tabid/2551/Default.aspx**, (accessed April 2024).

52 Y. Xu, Q. Ou, J. P. V. D. Hoek, G. Liu and K. M. Lompe, Photo-oxidation of Micro- and Nanoplastics: Physical, Chemical, and Biological Effects in Environments, *Environ. Sci. Technol.*, 2024, **58**(2), 991–1009, DOI: **10.1021/acs.est.3c07035**.

53 X. Wu, P. Liu, H. Wang, H. Huang, Y. Shi, C. Yang and S. Gao, Photo aging of polypropylene microplastics in estuary water and coastal seawater: Important role of chlorine ion, *Water Res.*, 2021, **202**, 117396, DOI: **10.1016/j.watres.2021.117396**.

54 M. Tsunooka, Mechanism of polymer deterioration, *Nippon Gomu Kyokaishi*, 1995, **68**(5), 274–283, DOI: **10.2324/gomu.68.274**.

55 Y. Nakayama, *Crosslinking reaction handbook*, Maruzen Publishing Co., Ltd., 2013, pp. 1–406.

56 M. Tsunooka and M. Shirai, *Crosslinking and decomposition of polymers - Aiming for environmental conservation*, CMC Publishing Co., Ltd., 2004, pp. 14–22.

57 Z. Osawa, *Polymer Deterioration/Long Life Handbook*, Maruzen Publishing Co., Ltd., 2011, p. 215.

58 K. Ikuta, K. Takao, Y. Matsumoto, S. Yukioka, H. Kataoka and S. Tanaka, Evaluation Method for Microplastics Deterioration Degree Using UV-Irradiated Polyethylene Model Sample, *Bunseki Kagaku*, 2022, **71**(10.11), 589–593, DOI: **10.2116/bunsekikagaku.71.589**.

59 *UBE Scientific Analysis Laboratory, Inc.*, **https://www.ube.co.jp/usal/documents/c004_141.htm**, (accessed April 2024).

60 I. Grigoriadou, K. M. Paraskevopoulos, M. Karavasili, G. Karagiannis, A. Vasileiou and D. Bikiaris, HDPE/Cu-nanofiber nanocomposites with enhanced mechanical and UV stability properties, *Composites, Part B*, 2013, **55**, 407–420, DOI: **10.1016/j.compositesb.2013.07.002**.

This journal is © The Royal Society of Chemistry 2025

Environ. Sci.: Nano, 2025, **12**, 1107–1115 | **1115**